Brain network metric derived from DWI: application to the limbic system

Luis Manuel Colon-Perez[1], Caitlin Spindler[2], Shelby Goicochea[3], William Triplett[4], Mansi Parekh[5], Eric Montie[6], Paul Richard Carney[5,7], and Thomas Mareci[4]
[1]*Physics, University of Florida, Gainesville, Florida, United States,* [2]*Biology, University of Florida,* [3]*Chemistry, University of Florida,* [4]*Biochemistry & Molecular Biology, University of Florida,* [5]*Pediatrics, University of Florida,* [6]*Science and Mathematics, University of South Carolina Beaufort, Bluffton, South Carolina, United States,* [7]*Wilder Center of Excellence for Epilepsy Research, University of Florida*

Introduction: Recent brain connectivity metrics derived from diffusion-weighted magnetic resonance imaging (DWI) allow for non-invasive study of brain structure[1,2]; however, such MRI derived measurements are inherently discrete and are affected by the resolution of acquisition. Nonetheless, with an appropriate normalization one can employ DWI and tractography to create measurements independent of image resolution and tractography algorithm. Many of the described brain networks derived from MRI in literature are simple graphs devoted to studying degree distribution and derived statistics from the degree distribution. Here we present an edge weight (EW) metric used to define the connectivity strength of a node, that would allow a better understanding of *local* networks relevant to any specific form of pathology, e.g. limbic epilepsy [3]. The EW defined here focuses on the fibrous structure of the brain to describe the network rather than the node degree based distribution that arises from random cortical segmentation[2]. With this EW metric, anatomical structures are defined, i.e. nodes, and the implied white matter tracts from tractography give rise to the edge, allowing the creation of a weighted network.

Methods: HARDI data from 4 excised rat brains was acquired using a Bruker 17.6T magnet with a diffusion spin echo sequence and isotropic resolution of 190 μm^3. We used an electrostatic equilibrium analogy scheme to uniformly distribute the diffusion weighting directions[4]. The diffusion displacement probability within each voxel was estimated using the method of Wishart (MOW)[5] distributions. Fiber tracks were calculated by seeding all voxels and by following fibers with the FACT algorithm[6] using a tracking step size of no more than 0.5 voxel length. The calculation of the network is a two-step process to define the edge weight, see eq. 1. In the *first step,* the set of all fibers passing through any two ROIs defines a set of *M* voxels that contain the fibers connecting the ROIs, see fig. 1c. In the *second step*, only the fibers that originated from the *M* voxels and the area defined by the fibers that make up the edge, see fig. 1d, is used to calculate the EW.

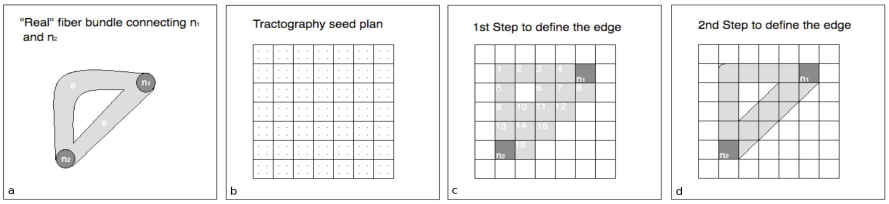

Figure 1. Diagram of the algorithm that selects the fibers that make up the edge. (a) Sketch of the "real" fiber bundle to be analyzed through the MR based edge weight. (b) Tractography seed plan used. Every voxel in the image is seeded homogenously, spreading the seed points through the entire image. (c) The 1st step is to define the edge to be able to verify which voxels lie in the fiber path that makes up the edge. (d) The 2nd step is to verify which seed points lie in the actual fiber path and calculate the edge weight.

$$w(e_{ij}) = \left(\frac{V_{voxel}}{P_{voxel}}\right)\left(\frac{2}{A_i+A_j}\right)\sum_{m=1}^{M}\sum_{p=1}^{P}\frac{\delta(x-x_{p.m})\delta(y-y_{p,m})\delta(z-z_{p.m})}{l(f_{p,m})} \quad (1), \qquad s(n_i) = \sum_{i\neq j} w(e_{ij}) \quad (2)$$

The coordinates in the delta functions are selective of points that lie within the *M* voxels making up the edge, (fig. 1c) and on the *p* seed points within voxel *m* (fig. 1b) that lie in the region that makes up the edge (fig. 1d). The node strength, eq. 2, for node *i* is derived directly from the edge weight by summing the weights of the edges that connect other nodes to node *i.*

Results: The EW, $w(e_{ij})$, and node connection strength, $s(n_i)$, were calculated. The described edge weight resulted in a 62.5% decrease in fibers compared to the EW calculated when the 2nd step described in the methods was disregarded. Because fiber tracking is performed throughout the entire brain, most of the calculated fibers that connect any two ROIs originate within the ROIs themselves or another white matter (WM) track. Therefore, if the 2nd step is disregarded the EW may not actually represent a measure of WM structure. The variability of the EW displays a decrease on the order of about 10% to 26% for most edges when applying the 2nd step.

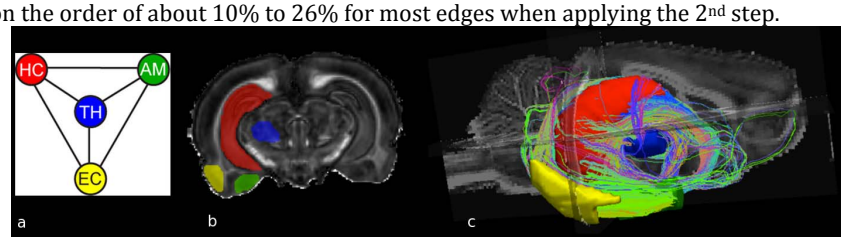

Figure 2. Limbic system network; hippocampus (HC), thalamus (TH), amygdala (AM) and entorhinal cortex. (a) Limbic system graph. (b) Coronal slice displaying the ROIs, or nodes, in the network. (c) Output network, each fiber passes through any two ROIs.

Conclusion: In this work we present a weighted brain network metric that allows the study of specific fibrous structures of the brain, which is independent of resolution and tractography algorithms; however the nature of the discrete geometry in MRI is the primary limitation to applying this measure. In particular, the effect of volume averaging may limit the accuracy of edge length determination (using Eq. 1), which alters the network results of the edge weight. Since many of the WM tracts connecting the limbic structures are small, DWI at lower resolutions may not capture many of these small tracks, which may also be confounded by volume averaging with GM as will as other WM tracts. Therefore, for small fiber paths high resolution scans should be obtained to accurately map the WM tracks.

References: **(1)** Sporns, O. Tononi, G.; Kötter, R. *PLoS computational biology* **2005**, *1*, e42. **(2)** Hagmann, P. Kurant, M. Gigandet, X. Thiran, P. Wedeen, V. J. Meuli, R.; Thiran, J.-P. *PloS one* **2007**, *2*, e597. **(3)** Bertram, E. H. *Epilepsy & Behavior* **2009**, *14*, 32–37. **(4)** Jones, D.; Horsfield, M. *Magnetic Resonance in Medicine* **1999**, *42*, 515-25. **(5)** Jian, B. Vemuri, B. C. Ozarslan, E. Carney, P. R.; Mareci, T. H. *NeuroImage* **2007**, *37*, 164-76. **(6)** Mori, S. Crain, B. J. Chacko, V. P.; van Zijl, P. C. *Annals of neurology* **1999**, *45*, 265-9.